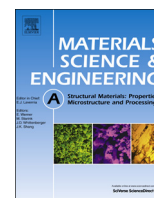




ELSEVIER

Contents lists available at ScienceDirect

## Materials Science &amp; Engineering A

journal homepage: [www.elsevier.com/locate/msea](http://www.elsevier.com/locate/msea)

# Grain-orientation-dependent of $\gamma$ - $\epsilon$ - $\alpha'$ transformation and twinning in a super-high-strength, high ductility austenitic Mn-steel

M. Eskandari<sup>a,\*</sup>, A. Zarei-Hanzaki<sup>b</sup>, M.A. Mohtadi-Bonab<sup>c</sup>, Y. Onuki<sup>d</sup>, R. Basu<sup>e</sup>, A. Asghari<sup>f</sup>, J.A. Szpunar<sup>g</sup>

<sup>a</sup> Department of Materials Science & Engineering, Faculty of Engineering, Shahid Chamran University of Ahvaz, Ahvaz, Iran

<sup>b</sup> Hot Deformation & Thermo-mechanical Processing of High Performance Engineering Materials, School of Metallurgy and Materials Engineering, University of Tehran, Tehran, Iran

<sup>c</sup> Department of Mechanical Engineering, University of Bonab, Velayat Highway, Iran

<sup>d</sup> Frontier Research Center for Applied Atomic Sciences, Ibaraki University, Japan

<sup>e</sup> Department of Mechanical Engineering, IITM University, Gurgaon, India

<sup>f</sup> Electrical and Computer Engineering Department, University of Texas at San Antonio, Texas, United States

<sup>g</sup> Advanced Materials for Clean Energy, Department of Mechanical Engineering, University of Saskatchewan, Canada

## ARTICLE INFO

## Article history:

Received 30 April 2016

Received in revised form

31 July 2016

Accepted 6 August 2016

Available online 7 August 2016

## Keywords:

Austenitic steel

Deformation

Orientations

EBSD

## ABSTRACT

A newly developed, austenitic lightweight steel, containing a low-density element, Al, exhibits tensile elongation up to 50% as well as high ultimate-tensile stress (tensile fracture at 1800 MPa) without necking behavior. Electron backscatter diffraction analysis is carried out to investigate the orientation dependence of the martensitic transformation in tensile testing to 30% strain at 323 K (25 °C). A pronounced  $\gamma \rightarrow \epsilon \rightarrow \alpha'$  transformation is observed in  $\langle 111 \rangle$  and  $\langle 110 \rangle$  ||TD (TD: tensile direction)  $\gamma$ -grains. The  $\alpha'$ -transformation textures is analyzed. Large misorientation spreads is seen in the  $\langle 100 \rangle$  ||TD  $\gamma$ -grains. Interestingly, twin-assisted martensitic transformation is detected in the  $\langle 111 \rangle$  ||TD followed by the twin boundary directly moving to a  $\gamma/\alpha'$  phase boundary. These phenomena are related to a change of Schmid factor for different orientations of grains.

© 2016 Elsevier B.V. All rights reserved.

## 1. Introduction

Recently, new groups of Mn-steels such as transformation induced plasticity (TRIP) steels and twinning induced plasticity (TWIP) steels have attracted special attention due to their good combination of high strength and ductility [1–6]. In general, the deformation mechanisms of such steels are linked to the mechanical stability of austenite and may change with the content of Mn due to a change in the stacking fault energy (SFE) [6–8]. In low-Mn (3–4 wt%) duplex steels [9], the only TRIP mechanism was seen in a medium-Mn (8–10 wt%) duplex steel [10], where both TRIP and TWIP mechanisms can work. Under this condition, an excellent combination of strength and ductility are achieved. For example, the mechanical properties of this steel are such that the tensile elongation was tested up to 77% and the tensile strength was 734 MPa.

It has been established that the SFE of the austenite is not the most important parameter affecting deformation mechanisms in Mn-steel [11]. It has also been shown that both martensitic

transformation and deformation twinning are closely related to the orientation of FCC grains along the stress direction [12–14]. For instance,  $\langle 110 \rangle$  ||TD oriented austenite is more prone to martensitic transformation in a TRIP steel while  $\langle 111 \rangle$  ||TD oriented austenite showed pronounced twinning in a TWIP steel during tensile deformation. There is, therefore, significant local inhomogeneity of plastic deformation in steel due to different orientations of FCC grains. In a specific range of SFE, in which TRIP and TWIP are concurrently activated, the role of grain orientation on the deformation mechanism is crucial. A very complex microstructure may be formed in the austenite phase. It is reported [15] that if martensite forms earlier, the twinning may be postponed at the vicinity of the martensite due to stress relaxation. On the other hand, where twins are first formed, this can expedite or put off the martensitic transformation owing to local changes in texture of the austenite. Such local texture may be represented by hard or soft orientations with different Schmid factors [16]. Moreover, twin boundaries are considered as the nucleation sites and can trigger martensite formation.

It is therefore of great interest to investigate the twin and martensite formation in FCC grains that have different orientations, i.e., different Schmid factors. The question to be asked is how grain orientations influence the formation of strain-induced

\* Corresponding author.

E-mail addresses: [m.eskandari@scu.ac.ir](mailto:m.eskandari@scu.ac.ir), [m.eskandari@ut.ac.ir](mailto:m.eskandari@ut.ac.ir) (M. Eskandari).

martensite and twins in low to high Mn-steels. As such information is not available [17–19], especially in the case of Mn steel, this study addresses this question for a super-high-strength austenitic lightweight steel with 20 (wt%) Mn. For this purpose, crystal-orientation maps are acquired for steel that are tensile-tested at 323 K (25 °C) up to 30 pct strain. Detailed deformation mechanisms in relation to the microstructural evolution are investigated by electron back-scattered diffraction (EBSD) analysis, and the correlation between microstructural evolution and grain orientation of austenite is verified. The corresponding  $\alpha'$ -transformation textures are calculated for each  $\gamma$ -grain orientation, taking the presence of  $\epsilon$ -martensite into account. Special attention is paid to the strain-induced martensite in  $\langle 100 \rangle$  ||TD oriented austenitic grains.

## 2. Experimental procedure

### 2.1. Materials

The experimental material was received in as-hot-rolled condition with chemical composition of Fe-0.11C-21Mn-2.50Si-1.60Al-0.02 Nb-0.02Ti-0.01 V (wt%). The hot-rolled microstructure consists of 99.5% austenite phase with a grain size of  $40 \pm 9 \mu\text{m}$ . The true stress-true strain behavior of the steel is measured using a Gotech AI-7000 universal testing machine at 323 K (25 °C) under a constant strain rate of  $0.001 \text{ s}^{-1}$ . The tensile tests are conducted according to the ASTM E08 standard with a specimen gauge length of 34 mm. The tensile axis is parallel to the sheet rolling direction (RD). To study the microstructural evolution, a tensile test is interrupted after straining to 0.3. Moreover, a deformed specimen is annealed at 1048 K (750 °C) for 60 s to compare its microstructure with a deformed one not annealed. The X-ray measurement is carried out using a Bruker D8 diffractometer with Cr K $\alpha$  radiation. In addition, the actual martensite content is determined using a Ferriteoscope model MP30 and considering the following equation [20]:

$$\text{Vol. \% martensite} = 1.75 \times \text{Ferriteoscope reading} \quad (1)$$

### 2.2. Preparation for EBSD

The microstructural analysis is performed using a Hitachi SU6600 field emission scanning electron microscope (FE-SEM), equipped with a Nordlys Nano Oxford detector of electron back-scattered diffraction (EBSD), which can operate at a voltage of 20. The specimens are mechanically polished with SiC papers followed by electro-polishing to prevent formation of  $\alpha$  or  $\epsilon$ -martensite

during sample preparation. The patterns are acquired using the AZTEC 2.0 data acquisition software compatible with the EBSD detector with a binning of  $4 \times 4$  pixels and a minimum of 6 bands for pattern recognition using acquisition rates (20 frames/s). The EBSD raw data are further analyzed using the Oxford Instruments Channel 5 post processing software.

## 3. Results and discussions

### 3.1. Initial microstructure and stress-strain curve

Fig. 1a shows the initial microstructure of the as-hot-rolled material. The material has a moderate grain size of  $40 \pm 9 \mu\text{m}$  with few annealing twins. The X-ray diffraction spectrum for the as-hot-rolled specimen (Fig. 1b) confirms the presence of only one phase, the austenite phase. Fig. 2 shows the tensile flow behavior of the material at 323 K (25 °C) under a strain rate of  $0.001 \text{ s}^{-1}$ . Considering the engineering stress-strain curve (Fig. 2a), this alloy does not exhibit significant necking during deformation at 323 K (25 °C). Therefore, the term fracture stress is used instead of ultimate tensile stress, for this steel. Fig. 2b shows that the experimental steel exhibited high fracture strength of about  $1810 \pm 10 \text{ MPa}$  and continuous yielding with a yield stress of  $450 \pm 10 \text{ MPa}$ . A linear strain hardening is seen up to final fracture. The final fracture appeared at engineering strain of about 0.60. The Ferriteoscope study displays that after fracture, the volume fraction of strain-induced  $\alpha'$ -martensite reached 40%.

### 3.2. Microstructure of tensile specimen after straining to 0.3

Fig. 3 depicts the microstructure in an austenite grain after straining to 0.3 (true strain). Fig. 3b shows the orientation map of the FCC austenite phase and the gray color corresponds to martensite. As observed in this map, the austenite grain is divided into three regions with different orientations  $\parallel$ TD ( $\{111\}$ : region 1,  $\{100\}$ : region 2 and  $\{110\}$ : region 3). According to pole figure analysis of these regions, as shown in Fig. 3c, the regions 1,2 and 2,3 display a twin relationship. The shape of the twin leads us to speculate that this is an annealing twin, which was formed in the hot-rolled specimen.

Fig. 3d shows there is no similarity of martensitic transformation (HCP  $\epsilon$ -martensite as yellow color and BCC  $\alpha'$ -martensite as blue color). As shown, regions 1 ( $\langle 111 \rangle$ -oriented) and 3 ( $\langle 110 \rangle$ -oriented) reveal much higher volume fractions of martensite than region 2 ( $\langle 100 \rangle$ -oriented). It is notable that the neighboring grain of the mentioned austenite grain, seen in region 4 with the same orientation ( $\langle 100 \rangle$ ), displays a different

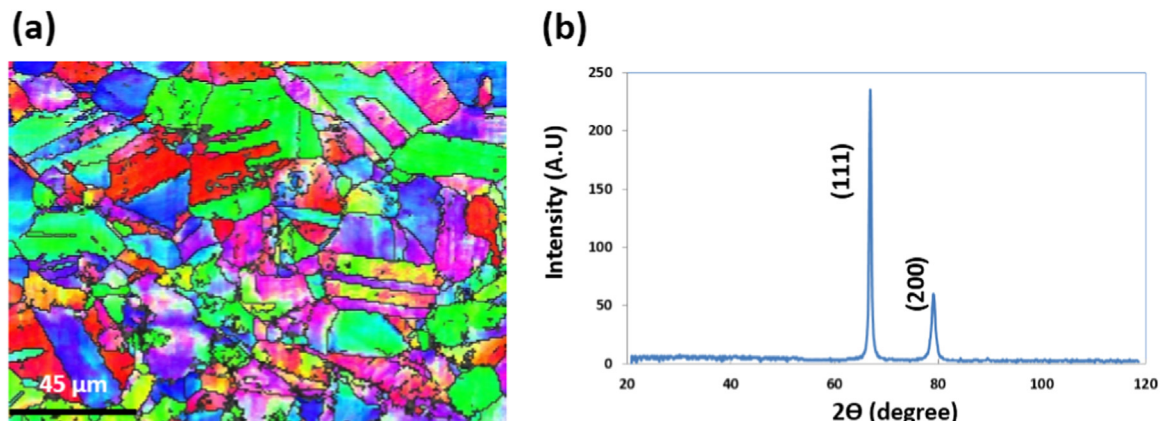


Fig. 1. (a) Initial microstructure of as-hot-rolled material, (b) X-ray diffraction of initial material.

Download English Version:

<https://daneshyari.com/en/article/7975035>

Download Persian Version:

<https://daneshyari.com/article/7975035>

[Daneshyari.com](https://daneshyari.com)